

## Ionization Dynamics versus Laser Intensity in Laser-Driven Multiply Charged Ions

H. G. Hetzheim\* and C. H. Keitel†

*Max-Planck-Institut für Kernphysik, Saupfercheckweg 1, 69117 Heidelberg, Germany*

(Received 8 August 2008; published 26 February 2009)

A sensitive method is put forward to determine the intensity of ultrastrong and short laser pulses via multiply charged ions. For guiding this experimentally challenging task, the laser-induced dynamics of these ions is calculated using both the classical relativistic and quantum Dirac equations. The resulting ionization yields and angular distributions are then evaluated to most sensitively deduce the applied maximal laser pulse intensity.

DOI: 10.1103/PhysRevLett.102.083003

PACS numbers: 32.80.Fb, 31.30.J-, 41.75.Jv, 42.65.-k

Profound insight into fundamental ultrahigh-field laser-matter interactions [1] requires an increase in the maximum intensity [2] and a decrease of the minimum pulse duration [3] of currently available lasers. The next generation of such laser pulses are envisaged to reach peak intensities of up to  $10^{23}$ – $10^{26}$  W/cm<sup>2</sup> [4]. Current high-power laser fields have been employed, for example, in laser acceleration [5], coherent x-ray generation, and  $\gamma$ -ray emission [6]. These ultraintense laser fields provide insights into the fascinating field of strong laser-matter interactions, e.g., to test the validity of QED through vacuum polarization [7], to study nuclear interaction and generating GeV electron beams [8], or for medical applications in cancer therapy [9].

Measuring the intensity of less powerful lasers simply involves recording the power and beam spot size. For ultrahigh laser intensities, however, this technique becomes less viable because the mirrors involved in the measurement process may not sustain such intensities anymore [2]. Moreover, the tighter focus of the laser pulse and the associated temporally and spatially sensitive distortion of the wave front [2] has to be taken into account, rendering the task very challenging. Instead of direct measurements, which are feasible for relatively low laser intensities, we consider indirect techniques using multiply charged ions to characterize ultraintense laser fields. These techniques provide a measure of the laser field amplitude as the multiply charged hydrogenlike ion can be chosen such that the atomic field strength is on average comparable to that of the laser field. The ionization of the ions [10] will depend both on the ionic field strength and the maximal laser intensity. The ease of selectively generating multiply charged hydrogenlike ions of any charge [10] renders them applicable to probe a wide range of laser intensities.

The central interest of this Letter is to develop a procedure to determine with optimal precision the maximal laser field strength of ultrastrong short pulses especially between  $10^{18}$  and  $10^{26}$  W/cm<sup>2</sup>. We show, based on relativistic classical trajectory Monte Carlo simulations, how a particular hydrogenlike ion is identified to most sensitively determine the applied laser field strength via measuring the fraction of over-the-barrier ionization (OTBI). The classi-

cal simulations are known to be in good agreement with the corresponding quantum calculations in the OTBI regime for the employed low laser frequencies and depend only to a rather small degree on the length and carrier phase of the short pulse of a few femtoseconds. Additionally, the ionization angle of the ejected electron [11] is investigated by the full quantum mechanical solution of the Dirac equation for laser-matter interaction in two dimensions [12]. As a consequence the laser field strength is linked to the ionization direction of the ejected electron as an alternative measurement technique.

The solution of the classical equation of motion for an electron in a Coulomb potential and a laser field can generally be calculated by employing a Monte Carlo simulation of the classical trajectories [13]. The fully relativistic three-dimensional extension can be found in [14]. The stationary ground state of the hydrogenlike ion is modeled by a microcanonical ensemble in phase space. The relativistic treatment of the electron is essential for high nuclear charge  $Z$  of hydrogenlike ions as the kinetic energy of the electron becomes non-negligible to its rest mass. Therefore, the energy of the ground state of the ion needs to be treated relativistically and is given by  $E_g = c^2\sqrt{1 - (Z\alpha)^2}$ , with  $\alpha = 1/c$  and speed of light  $c$ . Throughout this Letter, if not stated otherwise, atomic units are used ( $\hbar = m_e = |e| = 1$ ) with electron charge  $e$  and mass  $m_e$ . The relativistic equations of motion of the electron are solved numerically by the Runge-Kutta method with variable step size, given by

$$\dot{\mathbf{r}} = \frac{1}{\gamma} \mathbf{p}, \quad \dot{\mathbf{p}} = -\left(\mathbf{E}(\mathbf{r}, t) + \frac{1}{c\gamma} \mathbf{p} \times \mathbf{B}(\mathbf{r}, t)\right), \quad (1)$$

where  $\mathbf{E}(\mathbf{r}, t) = -\frac{1}{c} \frac{\partial \mathbf{A}(\mathbf{r}, t)}{\partial t} - \nabla \phi(r)$ ,  $\phi(r) = Z/r$ ,  $\mathbf{B}(\mathbf{r}, t) = \nabla \times \mathbf{A}(\mathbf{r}, t)$ , and  $\mathbf{A}(\mathbf{r}, t) = \frac{cE_0}{\omega} \cos(\omega t - \frac{\omega}{c} z) \mathbf{e}_x$  with time  $t$ , laser frequency  $\omega$ , maximal electric field strength  $E_0$ , and spatial components  $x, z$  in polarization and propagation direction, respectively,  $\gamma = \sqrt{1 + |\mathbf{p}|^2/c^2}$ , electron momentum  $\mathbf{p}$ , and position  $\mathbf{r}$ , with  $r = |\mathbf{r}|$ .

The solutions of the relativistic equations of motion are obtained by using step-by-step integration of the equations of motion Eq. (1). We averaged over 1000 test particles,

corresponding to different initial conditions randomly chosen from a microcanonical ensemble, prepared to be in the ground state of the selected hydrogenlike ion with ground state energy  $E_g$ . Trajectories with very small radii which “fall” into the core need to be excluded. The frequency of the linearly polarized single-cycle field was chosen such that it matches an experimental standard laser wavelength of  $\lambda = 1054$  nm. The main observable of interest, the ionization fraction, is calculated as the fraction of ionized trajectories to the total number of trajectories. An electron is considered ionized when its energy  $\mathcal{E}_m(t) = (\gamma - 1)c^2 - Z/r$  measured at the end of the laser pulse is positive. The ionization fraction depends mainly on the maximal laser intensity and frequency as well as to a smaller extent on the carrier phase, the shape, and the duration of the pulse. For an ion of, e.g.,  $Z = 20$ , variations in the pulse length from one to a few cycles or in the carrier phase by around  $\pi/4$  lead to changes in the ionization fraction of the order of 30% with a similar error in the associated laser intensity. More realistic pulses, e.g., containing a  $\sin^2$  envelope function, to mimic the turn-on and turn-off of the pulse, result in deviations in the ionization yield and the associated maximal laser intensity of the order of 2. Quantitative non-negligible deviations due to QED and other quantum effects are also likely to result especially starting at about  $Z = 50$ , rendering our evaluations, however, still useful for order of magnitude estimations. A detailed analysis of especially the dependence of the pulse shape and laser frequency on the ionization fraction will be published elsewhere [15].

The procedure for determining ultrastrong laser fields is described in the following. It is based on the measurement of the ionization fraction, which is a well-established experimental technique. The ionization fraction for several ions is given in Fig. 1. For a fixed  $Z$  the ionization fraction starts off with a flat profile followed by a rather steep rise ending up with a plateau of complete ionization. The sharp ascent of the ionization curve is the region where the ionization fraction can be most accurately measured. If an approximate laser intensity range may be expected, an ionic charge should be selected with maximal slope at this intensity. In case of a mistaken choice, e.g., if an ionization fraction of nearly 1 is measured, no precise statement about the corresponding intensity can be accomplished as the curve is effectively uniform. In this region several laser intensities can be associated with the same ionization fraction. Then our procedure requires that the ionic charge needs to be increased and vice versa for the range around a very small ionization fraction. This procedure needs to be continued until the ionization fraction is in the narrow range of the sharp ascent of the ionization curve (narrow intensity range), where the corresponding laser intensity can be most precisely determined.

At the steepest points of the sharp ascents for all investigated  $Z$  we can read off the ionization fraction and laser intensity for each curve in Fig. 1 and obtain Fig. 2. The unknown laser intensity can now be more effectively de-

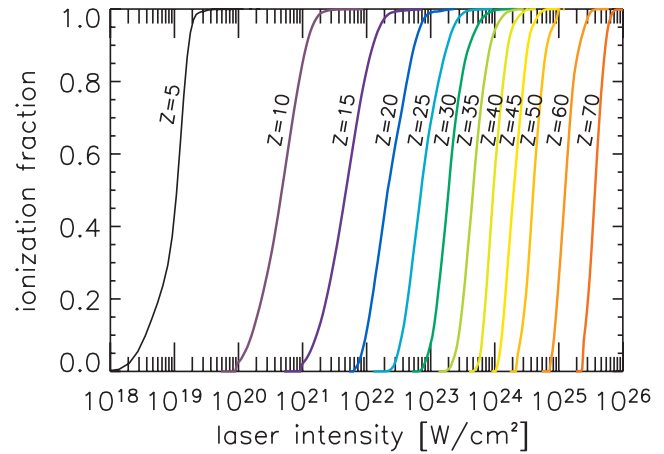


FIG. 1 (color online). The ionization fraction for several different hydrogenlike ions with nuclear charge  $Z$  as function of the maximal laser intensity in the laboratory frame is plotted. The ionization fraction is calculated at the end of a single-cycle square-shaped laser pulse of wavelength  $\lambda = 1054$  nm.

termined. In a first step, a particular ion needs to be selected, whose ionization fraction should then be measured. As a possible first guess, we refer to the dashed line of Fig. 2, which indicates the corresponding ionic charge of the expected intensity range. Here, for example, an intensity of  $I = 10^{23}$  W/cm<sup>2</sup> corresponds to a nuclear charge of  $Z = 30$ , which would be a proper candidate to begin with if an intensity around  $10^{23}$  W/cm<sup>2</sup> is assumed. In a second step, the ionization fraction of the selected fixed  $Z$  should be measured. If the ionization fraction is higher than the corresponding one depicted in Fig. 2 (solid line), then the measurement has to be repeated for a higher  $Z$  and vice versa for a smaller ionization fraction. This procedure

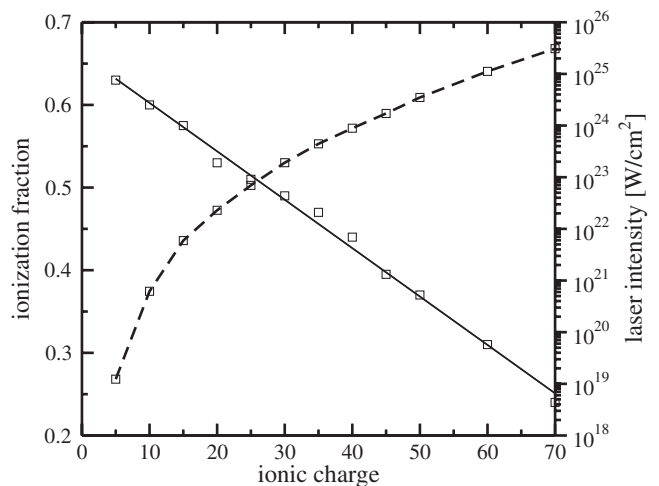


FIG. 2. The solid line defines the most sensitively measured ionization fraction (left axis), whereas the dashed line shows the corresponding laser intensity (right axis) as a function of the respective optimal  $Z$ . The laser field parameters are otherwise the same as given in Fig. 1. The lines are fits and the squares indicate the deduced points from Fig. 1.

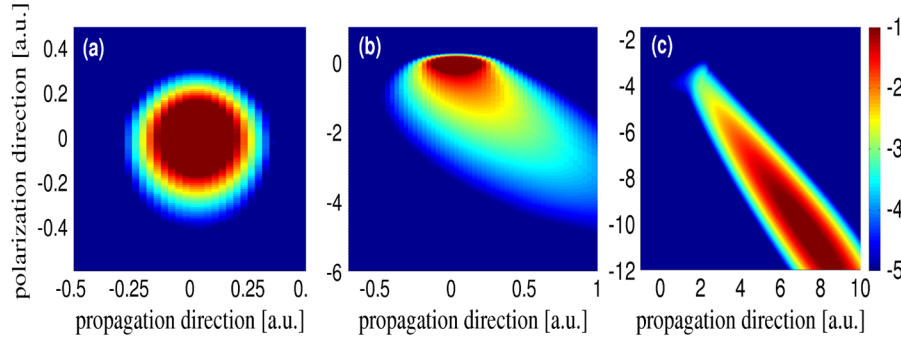


FIG. 3 (color online). Depicted are snapshots of the spatial electron probability density in the ion's rest frame on a logarithmic scale in the case of  $\text{Zn}^{29+}$  ( $Z = 30$ ) for different field strengths (a)  $\underline{E}_0 = 1000$  a.u. ( $E_0 = 16.67$  a.u.), (b)  $\underline{E}_0 = 2700$  a.u. ( $E_0 = 45.0$  a.u.), and (c)  $\underline{E}_0 = 10800$  a.u. ( $E_0 = 180.0$  a.u.) at  $1/10$  of the laser period in the ion's rest frame. Notice the different grid sizes which are due to the use of the adaptive grid approach [12] in order to handle the extremely large electron momenta. The hydrogenlike ion was assumed to be initially in the ground state.

needs to be continued until the ionization fraction matches with the corresponding value given by Fig. 2 for the respective ion. From the final  $Z$ , the corresponding laser intensity can then be read off via the dashed curve of Fig. 2.

A second independent criterion for the precise determination of ultrastrong laser intensities that has been performed originates from calculations on another observable, namely, the ionization angle. The following studies of the ionization with focus on the ionization angle are based as an alternative on the solution of the Dirac quantum equation of a bound electron in an ultrastrong laser field. The natural wave packet spreading of the ejected electron before it reaches the detector is therefore also well incorporated in the calculations. The Dirac equation reads

$$i \frac{\partial}{\partial t} \Psi(x, z; t) = \{c\boldsymbol{\alpha} \cdot \tilde{\mathbf{p}} + c^2\tilde{\beta} + U(x, z)\} \Psi(x, z; t). \quad (2)$$

The four component Dirac spinor wave function is represented by  $\Psi(x, z; t)$  with  $\boldsymbol{\alpha}$ ,  $\tilde{\beta}$  denoting the usual Dirac matrices, whereas the electron kinetic momentum is given by  $\tilde{\mathbf{p}} = \mathbf{p} + \frac{1}{c}\mathbf{A}(z; t)$ . The Dirac equation is solved numerically by applying the split-operator method [16]. The soft-core parameter  $a$  of the scalar potential  $U(x, z) = -(Z/\sqrt{x^2 + z^2 + a})$  models the missing third dimension and at the same time avoids the singularity of the Coulomb potential at its origin. It is chosen such that the ground state energy of the soft-core potential equals the corresponding ground state energy given by the analytical solution of the Coulomb potential. In our case of a nuclear charge  $Z = 30$ , the soft-core parameter is  $a = 0.0006$ . The laser field parameters are chosen to be the same as in Figs. 1 and 2. A further parameter taken into account is a possible preacceleration (here  $\gamma = 30$ ) of the ions opposite to the laser pulse, which may be adopted to optimal sensitivity with regard to the ionization angle.

The Dirac ground state of the ionic wave function as initially prepared is then propagated in time on a two-dimensional grid. The total energy of the electron  $\mathcal{E}$  including its rest mass  $c^2$  thereby needs to be temporally

resolved on a scale  $\Delta t \leq 1/\mathcal{E}$ , which renders the numerical calculation very lengthy in terms of computation time.

The determination of ultrastrong laser fields by the ionization angle  $\underline{\theta}$  in the ion's rest frame is calculated with respect to the laser propagation direction via the expectation value of the kinetic momentum of the electron in laser polarization direction  $\underline{p}_x$  and propagation direction  $\underline{p}_z$ , i.e., via  $\tan \underline{\theta} = \underline{p}_x / \underline{p}_z$ . The transformation of the ionization angle between the ion's rest and the laboratory frame is then carried out via

$$\tan \theta = \frac{\underline{p}_x}{\gamma(\underline{p}_z - \beta \sqrt{\underline{p}_x^2 + \underline{p}_z^2 + c^2})}. \quad (3)$$

For our calculations, the laser frequency  $\underline{\omega} = 2.58$  a.u. in the ion's rest frame ( $\omega = 0.043$  a.u.) and the parameter  $\beta$  are fixed, with  $\beta$  arising from a gamma boost of  $\gamma = 1/\sqrt{1 - \beta^2} = 30$ . These parameters can be chosen freely according to the experimental needs. The ionization angles of the emitted electron and the associated laser field strength in the ion's rest and laboratory frames are listed in Table I for  $\text{Zn}^{29+}$  ( $Z = 30$ ). In the OTBI regime a

TABLE I. The ionization angles in both the ion's rest frame  $\underline{\theta}$  and the laboratory frame  $\theta$  are given for different field amplitudes in the case of the hydrogenlike ion  $\text{Zn}^{29+}$  ( $Z = 30$ ). The values of the kinetic momentum for the calculation of the ionization angles were taken at  $1/8$  of the laser period of a single-cycle square-shaped pulse in the ion's rest frame. The underlined values are given in the ion's rest frame, whereas the values not underlined are indicated in the laboratory frame.

| $\underline{E}_0$ [a.u.] | $E_0$ [a.u.] | $\underline{p}_x$ [a.u.] | $\underline{p}_z$ [a.u.] | $ \underline{\theta} $ [deg] | $\theta$ [deg] |
|--------------------------|--------------|--------------------------|--------------------------|------------------------------|----------------|
| 1000                     | 16.67        | -1.20                    | 0.000094                 | 89.99                        | 179.98         |
| 2700                     | 45.0         | -6.14                    | 1.67                     | 74.78                        | 179.91         |
| 10800                    | 180.0        | -297.44                  | 327.77                   | 42.22                        | 175.80         |
| 16200                    | 270.0        | -444.29                  | 728.82                   | 31.36                        | 173.74         |
| 24000                    | 400.0        | -513.14                  | 968.83                   | 27.91                        | 172.79         |
| 32040                    | 534.0        | -560.46                  | 1158.30                  | 25.82                        | 172.11         |

corresponding classical trajectory Monte Carlo calculation shows an agreement with above Dirac results within an uncertainty of about 20%. Experimentally these measurements of ultrastrong laser fields can be confirmed with conventional intensities accessible today by taking advantage of the Doppler effect by means of counterpropagating an ion and a laser beam. The competing field strength of both the atom and the laser field can be clearly deduced from the dynamics of the electron density distribution. After leaving the vicinity of the nucleus, the electron is mainly influenced by the external laser field resulting in a large amplitude in polarization direction and an additional drift of the electron in propagation direction; see Fig. 3. These calculated snapshots were taken at 1/10 of the laser period, i.e., in the time range of a few ten attoseconds in the ion's rest frame. In the case of a low laser intensity as in Fig. 3(a), the major part of the electron density remains with the nucleus. However, with increasing laser field strength [Figs. 3(b) and 3(c)], the electron density close to the nucleus diminishes by moving away both in laser propagation and polarization direction, as governed by the high electron velocity and the Lorentz force.

The ionization angle  $\theta$  is reduced with increased laser intensity while keeping the ratio constant between the laser field strength  $E_0$  and the averaged electric field of the atomic ground state  $E_{\text{atom}} = Z^3$ . This shows the importance of the laser magnetic field component in ultrastrong fields yielding an enhanced relative momentum in the laser propagation direction with increasing intensity. Thus, following both from Figs. 1 and 2 and Table I, laser intensities of around  $10^{23}$  W/cm<sup>2</sup> may be sensitively measured with ions of  $Z = 30$ . For laser intensities of the order of  $10^{24}$ – $10^{25}$  W/cm<sup>2</sup>, which are feasible within the next few years [4], ions with charge  $Z = 40$ – $60$  are suitable according to Figs. 1 and 2.

In summary, we have performed classical relativistic and quantum Dirac calculations for the interaction of multiply charged hydrogenlike ions with ultraintense single-cycle laser pulses. Our studies of the ionization fraction and angular distribution of the ejected electron in the OTBI regime show that these observables can be employed to most sensitively determine the maximal laser pulse intensity of ultrastrong fields. In particular, taking advantage of the wide range of mean electric field strengths of multiply charged ions renders our method also suitable to somewhat higher laser intensities and to frequencies of x-ray free-electron lasers.

We acknowledge helpful discussions with Heiko Bauke and Guido Mocken.

\*hetzheim@mpi-hd.mpg.de

†keitel@mpi-hd.mpg.de

- [1] G. A. Mourou, T. Tajima, and S. V. Bulanov, *Rev. Mod. Phys.* **78**, 309 (2006); Y. I. Salamin *et al.*, *Phys. Rep.* **427**, 41 (2006); M. Marklund and P. Shukla, *Rev. Mod. Phys.*

- 78**, 591 (2006); A. Maquet and R. Grobe, *J. Mod. Opt.* **49**, 2001 (2002); C. H. Keitel, *Contemp. Phys.* **42**, 353 (2001).
- [2] S.-W. Bahk *et al.*, *Opt. Lett.* **29**, 2837 (2004); Y. Yanovsky *et al.*, *Opt. Express* **16**, 2109 (2008).
- [3] N. M. Naumova *et al.*, *Phys. Rev. Lett.* **92**, 063902 (2004); Y. Mairesse *et al.*, *ibid.* **93**, 163901 (2004).
- [4] European Light Infrastructure Scientific Case, <http://www.extreme-light-infrastructure.eu/>; High Power laser Energy Research (HiPER), Technical Background and Conceptual Design Report, <http://www.hiperlaser.org/docs/tdr/HiPERTDR2.pdf>.
- [5] S. P. D. Mangles *et al.*, *Nature (London)* **431**, 535 (2004); C. G. R. Geddes *et al.*, *ibid.* **431**, 538 (2004); J. Faure *et al.*, *ibid.* **431**, 541 (2004).
- [6] J. Seres *et al.*, *Nature (London)* **433**, 596 (2005); K. W. D. Ledingham *et al.*, *Science* **300**, 1107 (2003).
- [7] G. Brodin, M. Marklund, and L. Stenflo, *Phys. Rev. Lett.* **87**, 171801 (2001); T. Heinzl *et al.*, *Opt. Commun.* **267**, 318 (2006); A. Di Piazza, K. Z. Hatsagortsyan, and C. H. Keitel, *Phys. Rev. Lett.* **97**, 083603 (2006); **100**, 010403 (2008).
- [8] G. Pretzler *et al.*, *Phys. Rev. E* **58**, 1165 (1998); K. W. D. Ledingham *et al.*, *Phys. Rev. Lett.* **84**, 899 (2000); T. J. Bürvenich *et al.*, *Phys. Rev. Lett.* **96**, 142501 (2006); W. P. Leemans *et al.*, *Nature Phys.* **2**, 696 (2006); S. M. Pfotenhauer *et al.*, *New J. Phys.* **10**, 033034 (2008).
- [9] S. Fritzler *et al.*, *Appl. Phys. Lett.* **83**, 3039 (2003); H. Schwöerer *et al.*, *Nature (London)* **439**, 445 (2006); Y. I. Salamin *et al.*, *Phys. Rev. Lett.* **100**, 155004 (2008).
- [10] P. H. Mokler and T. Stöhlker, *Adv. At. Mol. Opt. Phys.* **37**, 297 (1996); E. M. Snyder *et al.*, *Phys. Rev. Lett.* **77**, 3347 (1996); J. Ullrich *et al.*, *J. Phys. B* **30**, 2917 (1997); T. Ditmire *et al.*, *Nature (London)* **386**, 54 (1997); S. J. McNaught *et al.*, *Phys. Rev. A* **58**, 1399 (1998); S. X. Hu and C. H. Keitel, *Phys. Rev. A* **63**, 053402 (2001); S. X. Hu and A. F. Starace, *Phys. Rev. Lett.* **88**, 245003 (2002); K. Yamakawa *et al.*, *Phys. Rev. A* **68**, 065403 (2003); V. P. Krainov, *J. Phys. B* **36**, 3187 (2003); V. S. Popov, *Usp. Fiz. Nauk* **174**, 921 (2004) [*Phys. Usp.* **47**, 855 (2004)]; J. R. Crespo López-Urrutia *et al.*, *J. Phys. Conf. Ser.* **2**, 42 (2004); K. Yamakawa *et al.*, *Phys. Rev. Lett.* **92**, 123001 (2004); E. Gubbini *et al.*, *Phys. Rev. Lett.* **94**, 053602 (2005); *J. Phys. B* **39**, S381 (2006); S. Palaniyappan *et al.*, *J. Phys. B* **39**, S357 (2006).
- [11] S. J. McNaught *et al.*, *Phys. Rev. Lett.* **78**, 626 (1997); C. I. Moore *et al.*, *Phys. Rev. Lett.* **82**, 1688 (1999); R. Taïeb *et al.*, *Phys. Rev. Lett.* **87**, 053002 (2001).
- [12] G. R. Mocken and C. H. Keitel, *J. Comput. Phys.* **199**, 558 (2004).
- [13] R. Abrines and I. C. Percival, *Proc. Phys. Soc. London* **88**, 861 (1966); J. S. Cohen, *Phys. Rev. A* **26**, 3008 (1982).
- [14] H. Schmitz, K. Boucke, and H.-J. Kull, *Phys. Rev. A* **57**, 467 (1998); L. N. Gaier and C. H. Keitel, *Phys. Rev. A* **65**, 023406 (2002).
- [15] H. G. Hetzheim *et al.* (to be published).
- [16] U. W. Rathe *et al.*, *J. Phys. B* **30**, L531 (1997); J. W. Braun, Q. Su, and R. Grobe, *Phys. Rev. A* **59**, 604 (1999); G. R. Mocken and C. H. Keitel, *Comput. Phys. Commun.* **178**, 868 (2008).